Journal of Nonlinear Modeling and Analysis
Volume 7, Number 1, February 2025, 1–19
https://journal.global-sci.org/jnma
DOI:10.12150/jnma.2025.1

Stability and Bifurcation Analysis for a Predator-Prey Model with Crowley-Martin Functional Response

Mengran Yuan[1,2], Na Wang[1,†]

Abstract This paper mainly focuses on the Gauze-type predator-prey model with Crowley-Martin functional response. The local stability of the equilibria is investigated by analyzing the characteristic equation and using the Routh-Hurwitz criterion. Besides, dynamic behavior has been studied by using the center manifold theorem and normal form theory. Finally, several numerical simulations not only verify the theoretical results of Hopf bifurcation but also display more interesting dynamical properties of the model.

Keywords Predator-prey system, Crowley-Martin functional response, Hopf bifurcation, center manifold theorem, normal form theory

MSC(2010) 34C23, 37C75, 37N25.

1. Introduction

Mathematical models in ecology provides us with information on the dynamical behavior of the ecological system. The interactions between predator and prey in nature are largely responsible for the rich biodiversity of complex ecosystems. So, it is necessary to analyse the predator-prey relationship qualitatively and quantitatively. The most paramount and critical term in the predator-prey model is the functional response function, which reflects the relationship between the predator population density and the prey population density. Most functional response functions depend either on the predator or the prey, such as classic Holling types functional response which were regarded as "prey-dependent" [5]. However, that is not entirely consistent with the actual situation in nature.

Let $x(t)$ and $y(t)$ denote densities of the prey and predators at time t, respectively. The classical Gauze-type predator-prey system without considering the spatial effect takes the following form [6]:

$$\begin{cases} x'(t) = xg(x) - yP(x,y), \\ y'(t) = \eta yP(x,y) - \mu y, \end{cases} \tag{1.1}$$

where $g(x) = r(1 - x/K)$, r is the growth rate of prey and K is called the carrying

†the corresponding author.
Email address: ymengran2388@126.com(M. Yuan), wangna1621@126.com (N. Wang)
[1]Department of Applied Mathematics, Shanghai Institute of Technology, Shanghai, China
[2]Department of Mathematics, China University of Mining and Technology, Beijing, China

capacity of prey. $P(x, y)$ indicates the consumption rate of prey by a predator or the functional response of the predator.

Skalski and Gilliam [20] separately studied three functional response functions that reveal the interaction between predator and prey, and obtained rich statistical evidence from 19 predator-prey ecosystems. Research indicates that the Crowley-Martin functional response performed better in the three. Since this functional response recognizes the rich and biologically reasonable dynamics [1, 21], it is necessary for us to study it.

The Cowley-Martin functional response considered in this article takes the following form

$$P(x, y) = \frac{mx}{(a + bx)(a + cy)}, \tag{1.2}$$

where m, a, b, c are positive constants that stand for the effects of consumption rate, saturation constant, handling time and the magnitude of interference among predators, respectively.

Over the past few decades, more and more information about the predator-prey system with Crowley-Martin functional response has been available [10, 14, 23, 24]. Zhou [26] presented qualitative analysis of the predator-prey model for Crowley-Martin functional responses. Li et al. [9] examined a predator-prey model with Crowley-Martin functional response for positive periodic solutions. Maiti et al. [12, 13] considered a prey-predator model which divides the scope of biological activity into two areas. They analysed the direction of Hopf bifurcation and the stability of the bifurcation periodic solution, and used the V function to judge the global stability of the time-delay system. Upadhyay and Naji [24] studied a three food chain system with Crowley-Martin functional response and got local and global stability for non-negative equilibrium, conditions for the persistence of the system and bifurcation diagrams. Shi et al. [19] considered a predator-prey model with Crowley-Martin function, they considered the locally asymptotic stability of nonnegative equilibria and obtained sufficient conditions for the global stability of the positive equilibrium. Saha [17] studied a predator-predator model with a small parameter ϵ which is a slow-fast system that causes singular perturbation problem in mathematics. Besides, Santra etc [18] investigated the dynamics of a discrete predator-prey model, focusing on the Neimark-Sacker bifurcation. Another important bifurcation of the discrete differential equation is the Flip bifurcation, so we will also study the Flip bifurcation corresponding to the discrete system.

In this paper, we consider a predator-prey system model with a small parameter ϵ, which is, the significant difference in population density between the predator and prey, such as spruce-budworm system [2, 11, 15, 22]. The main contributions of this work are summarized in the following.

(1) We carried out the stability analysis of the system, and determined the bifurcation parameter of the system as δ through mathematical analysis of the system model.

(2) We calculated the critical value δ_0 and verified that the system occurs Hopf bifurcation when δ passes δ_0 from right to left. We also analysed the direction of Hopf bifurcation and the stability of the bifurcation periodic solution.

(3) We also gave conditions for the corresponding discrete system to have a flip bifurcation.

(4) The example given in the numerical simulation is subcritical Hopf bifurcation, the bifurcating periodic solutions are stable and their period increases with

δ.

The rest of this paper is organized as follows. In the next section, we introduce the mathematical formula of the model and make brief analysis. In Section 3, We analyse the local stability of the equilibrium point and the conditions for the occurrence of hopf bifurcation. In Section 4, by using center manifold theorem and normal form theory, we judge the direction, stability and period of the periodic solution of the Hopf bifurcation. In Section 5, we analyse the conditions for the production of the Flip bifurcation. Numerical simulations are given in Section 6. Section 7 makes the conclusion to this paper.

2. The mathematical model

We consider the following predator-prey system model with Crowley-Martin functional response:

$$\begin{cases} \dfrac{\mathrm{d}u}{\mathrm{d}t} = ru(1-\dfrac{u}{K}) - \dfrac{muv}{(a+bu)(a+cv)}, \\ \dfrac{\mathrm{d}v}{\mathrm{d}t} = \dfrac{emuv}{(a+bu)(a+cv)} - nv, \end{cases} \tag{2.1}$$

where u and v represent prey population density and predator population density, respectively. The parameters r, K, m, a, b, c, n and e are all greater than 0. In system (2.1), r is the prey intrinsic growth rate, m is the consumption rate, K is the carrying capacity of the environment, a represents the saturation constant, b is the handling time, c stands for the magnitude of interference among predators, n is the predator's per-capita death rate, and e takes into account the efficiency of conversion of predation into biomass.

We assume that the death rate n and the conversion rate e are small. To be precise, we set n and e as sufficiently small parameters, e_1 as the rescaled conversion rate, and n_1 represents the rescaled predator death rate. We then have the slow-fast predator-prey system

$$\begin{cases} \dfrac{\mathrm{d}u}{\mathrm{d}t} = ru(1-\dfrac{u}{K}) - \dfrac{muv}{(a+bu)(a+cv)}, \\ \dfrac{\mathrm{d}v}{\mathrm{d}t} = \epsilon\left[\dfrac{e_1muv}{(a+bu)(a+cv)} - n_1v\right], \end{cases} \tag{2.2}$$

where $e = \epsilon e_1$,$n = \epsilon n_1$, and $0 < \epsilon \ll 1$.

Using the rescaling transformation to make system (2.2) dimensionless:

$$T = rt, x = \frac{u}{K}, y = \frac{cv}{bK}, \tag{2.3}$$

we have

$$\begin{cases} \dfrac{\mathrm{d}x}{\mathrm{d}T} = x(1-x) - \dfrac{\alpha xy}{(\delta+x)(\delta+y)}, \\ \dfrac{\mathrm{d}y}{\mathrm{d}T} = \epsilon\left[\dfrac{\beta xy}{(\delta+x)(\delta+y)} - \gamma y\right], \end{cases} \tag{2.4}$$

in which the new variables are x, y, and $\alpha = \frac{m}{bcrK},\ \beta = \dfrac{me_1}{rb},\ \gamma = \dfrac{n_1}{r},\ \delta = \dfrac{a}{bK}$.

The system (2.4) is topologically equivalent to model (2.5), and we replace T with t just out of habit,

$$\begin{cases} \dfrac{\mathrm{d}x}{\mathrm{d}t} = x(1-x)(\delta+x)(\delta+y) - \alpha xy = f(x,y), \\ \dfrac{\mathrm{d}y}{\mathrm{d}t} = \epsilon\left[\beta xy - \gamma y(\delta+x)(\delta+y)\right] = \epsilon g(x,y). \end{cases} \tag{2.5}$$

We will analyse system (2.5) with an initial value greater than 0. From the biological populations in nature, we only consider the dynamic behavior of the system (2.5) in the first quadrant of the $x-y$ plane, denoted by

$$\Omega = \{(x,y) \in R^2 : x \geq 0, y \geq 0\}. \tag{2.6}$$

Equation (2.5) has positive solutions with initial conditions (2.6), and the solutions of system (2.5) initiated from Int Ω are uniformly bounded. The proof process is similar to that given in Tripath [23].

Let $\tau = \epsilon t$. Then we obtain

$$\begin{cases} \epsilon\dfrac{\mathrm{d}x}{\mathrm{d}\tau} = x(1-x)(\delta+x)(\delta+y) - \alpha xy, \\ \dfrac{\mathrm{d}y}{\mathrm{d}\tau} = \beta xy - \gamma y(\delta+x)(\delta+y). \end{cases} \tag{2.7}$$

The dynamic behavior of the model (2.7) is restricted to the area Ω. The parameter ϵ can be regarded as the "separation" of time scales, that is, the ratio between the linear death rate of the predator density and the linear growth rate of the prey density. We call t and τ as the fast time scale and slow time scale respectively. For $0 < \epsilon \ll 1$, we refer to x and y as fast variables and slow variables, respectively.

Substituting $\epsilon = 0$ into system (2.5), we obtain the layer system or the fast system, which is given by

$$\begin{cases} \dfrac{\mathrm{d}x}{\mathrm{d}t} = x(1-x)(\delta+x)(\delta+y) - \alpha xy, \\ \dfrac{\mathrm{d}y}{\mathrm{d}t} = 0. \end{cases} \tag{2.8}$$

Substituting $\epsilon = 0$ into system (2.7), we get the slow system, which is differential algebraic equation given by

$$\begin{cases} 0 = x(1-x)(\delta+x)(\delta+y) - \alpha xy, \\ \dfrac{\mathrm{d}y}{\mathrm{d}\tau} = \beta xy - \gamma y(\delta+x)(\delta+y). \end{cases} \tag{2.9}$$

Equation (2.9) can be used to deduce $y = \varphi(x)$ where

$$\varphi(x) = \frac{\delta(1-x)(\delta+x)}{\alpha - (1-x)(\delta+x)}. \tag{2.10}$$

The slow flow is forced on the critical set:

$$\begin{aligned} M_0 &= \{(x,y) \in \Omega : f(x,y) = 0\} \\ &= \{(x,y) \in \Omega : x = 0 \ or \ y = \varphi(x), \alpha > (1-x)(\delta+x)\}, \end{aligned} \tag{2.11}$$

where $\varphi(x)$ is given by (2.10). It comprises two types of critical manifolds that are given by

$$M_{10} = \{(x, y) \in \Omega \mid x = 0\}, \tag{2.12}$$

$$M_{20} = \{(x, y) \in \Omega \mid y = \varphi(x) = \frac{\delta(1-x)(\delta+x)}{\alpha-(1-x)(\delta+x)}\}. \tag{2.13}$$

The integral curves of M_{10} are parallel to the horizontal axis which means that the predator population density remains steady on the first flow M_{10}. The flow (2.8) is a parametrized differential equation in x where y is regarded as a parameter. And, the equilibrium point of equation (2.8) is in one-to-one correspondence with the points in M_0. The dynamic behavior of flow M_{20} is determined by

$$\frac{dx}{d\tau} = \frac{\varphi(x)\{\beta x - \gamma(\delta+x)(\delta+\varphi(x)\}}{\varphi'(x)}, \tag{2.14}$$

where $\varphi'(x) = \dfrac{\alpha\delta(1-\delta-2x)}{[\alpha-(1-x)(\delta+x)]^2}$, and we get the following results on the critical manifold M_{20}.

Lemma 2.1. *The function $\varphi(x)$ has the following statements.*

1. *If $0 < x < \frac{1-\delta}{2}$, $\varphi(x)$ is strictly increasing in Ω; if $\frac{1-\delta}{2} < x < 1$, $\varphi(x)$ is strictly decreasing.*
2. *The function $\varphi(x)$ has a local maximum at $x_1 = \frac{1-\delta}{2}$.*

We focus our attention on the parametric condition

$$\alpha > (1-x)(\delta+x),\ \delta < 1. \tag{2.15}$$

In this case, M_{20} is a parabolic shape and consists of two branches S_0^r and S_0^a, where S_0^r is the branch from $P(0, \frac{\delta^2}{\alpha-\delta})$ to $Q(x_1, y_1)$; S_0^a is the branch from maximum point $Q(x_1, y_1)$ to $R(1, 0)$. P is the intersection of manifolds M_{10} and M_{20}. Thereby,

$$S_0^r = M_{20} \cap \{(x, y) \in \Omega \mid 0 < x \le x_1\}, \tag{2.16}$$

$$S_0^a = M_{20} \cap \{(x, y) \in \Omega \mid x_1 < x \le 1\}. \tag{2.17}$$

Theorem 2.1. *1. M_{20} is non-hyperbolic at $Q(x_1, y_1)$, $P(0, \frac{\delta^2}{\alpha-\delta})$.*

2. When the parameters hold the condition of (2.15), the branches S_0^r and S_0^a are hyperbolic repelling and hyperbolic attracting, respectively.

Proof. (i) We obtain $\frac{\partial f}{\partial x} = \frac{\alpha\delta x(1-2x-\delta)}{\alpha-(1-x)(\delta+x)}$ at point $(x, \varphi(x))$. Obviously, $\frac{\partial f}{\partial x} = 0$ at the points $Q(x_1, y_1)$ and $P(0, \frac{\delta^2}{\alpha-\delta})$. Therefore, $\frac{\partial f}{\partial x}$ has zero eigenvalue at these points and M_{20} looses its hyperbolicity at P and Q.

(ii) Evidently, $\frac{\partial f}{\partial x} > 0$ at point $(x, \varphi(x))$ for $x < x_1$, $\frac{\partial f}{\partial x} < 0$ at point $(x, \varphi(x))$ for $x > x_1$. That is, the branches are hyperbolic repelling and hyperbolic attracting, respectively. □

3. Stability of equiliburium and local Hopf bifurcation

We can get the reduced equation of system (2.7), which is

$$\begin{cases} x(1-x)(\delta+x)(\delta+y)-\alpha xy=0, \\ \beta xy-\gamma y(\delta+x)(\delta+y)=0. \end{cases} \tag{3.1}$$

Solving the equation (3.1) to get the equilibrium points, then we have the equilibrias $E_0(0,0)$, $E_1(0,\frac{\delta^2}{\alpha-\delta})$,$E_2(\frac{\gamma\beta}{\beta-\gamma\beta},0)$ and $E_4(1,0)$ on the coordinate axes, and non-trivial equilibria $E_3(x^*,y^*)$ where x^* is the positive root of the cubic equation

$$\beta x^3+\beta(\delta-1)x^2+(\alpha\beta-\alpha\delta\gamma-\beta\delta)x-\alpha\gamma\delta^2=0. \tag{3.2}$$

Lemma 3.1. *The equation* (3.2) *has at least one positive root.*

1. *If* $\alpha\beta-\alpha\delta\gamma-\beta\delta<0$*, then Eq* (3.2) *has a unique positive root,* (H_1)
2. *if* $\alpha\beta-\alpha\delta\gamma-\beta\delta>0$*, then Eq* (3.2) *has two positive roots.* (H_2)

In the ensuing discussion, we assume that equation (3.2) has only one positive root. In order to investigate the local stability of equilibrium, we calculate the Jacobian matrix of system (2.4) corresponding to each equilibrium point. The Jacobian matrix J of system (2.4) at any point (x,y) is given by

$$J=\begin{pmatrix} 1-2x-\dfrac{\alpha\delta y}{(\delta+x)^2(\delta+y)} & -\dfrac{\alpha\delta x}{(\delta+x)(\delta+y)^2} \\ \dfrac{\epsilon\beta\delta y}{(\delta+x)^2(\delta+y)} & \dfrac{\epsilon\beta\delta x}{(\delta+x)(\delta+y)^2}-\epsilon\gamma \end{pmatrix}.$$

(i) The equilibria $E_0(0,0)$ is always a saddle.

(ii) The equilibria $E_1(0,\dfrac{\delta^2}{\alpha-\delta})$ is non-hyperbolic, and the eigenvalues are $\lambda_1=0$ and $\lambda_2=-\epsilon\gamma$. E_1 is stable but not asymptotically stable.

(iii^a) The equilibrium point $E_2(\dfrac{\gamma\beta}{\beta-\gamma\beta},0)$ is locally asymptotically stable if $\gamma\delta<\beta<3\gamma\delta$, or $\dfrac{\beta}{(\beta-\delta^2+\delta)}>\gamma\delta$.

(iii^b) The equilibria E_2 is a saddle point with stable manifold locally in the x-direction and unstable manifold locally in the y-direction if $(\dfrac{\beta-3\gamma\delta}{\beta-\gamma\delta})[\dfrac{\beta}{\delta(\beta-\delta^2+\delta)}+\gamma]>0$.

(iv^a) The equilibrium point $E_4(1,0)$ is a saddle with stable manifold locally in the x-direction and with unstable manifold locally in the y-direction if $\dfrac{\epsilon\beta}{(\delta+1)\delta^2}>\epsilon\gamma$.

(iv^b) E_4 is stable if $\dfrac{\epsilon\beta}{(\delta+1)\delta^2}<\epsilon\gamma$, and when E_4 exists, the interior equilibrium point E_3 does not exist. That is, $E_4(1,0)$ is a global attracter for this condition, and all the trajectories initiating from $Int\Omega$ converge to E_4.

(v) Calculating the Jacobian matrix at the inner equilibrium $E_3(x^*,y^*)$, we have

$$J^*=\begin{pmatrix} 1-2x-\alpha Q & -\alpha R \\ \epsilon\beta Q & \epsilon\beta R-\epsilon\gamma \end{pmatrix},$$

where $Q = \dfrac{\delta y^*}{(\delta + x^*)^2(\delta + y^*)}$ and $R = \dfrac{\delta x^*}{(\delta + x^*)(\delta + y^*)^2}$.

Let the right-end item of Eq(2.4) equal to zero, and we obtain

$$x^* = \frac{\gamma}{\beta}(\delta + x)(\delta + y), \tag{3.3}$$

$$y^* = \frac{1 - x}{\alpha}(\delta + x)(\delta + y). \tag{3.4}$$

Substituting Eq (3.3) and (3.4) in the Jacobian matrix J^*, we get a more concise matrix

$$J^* = \begin{pmatrix} J_1 & J_2 \\ J_3 & J_4 \end{pmatrix},$$

where $J_1 = 1 - 2x^* - \dfrac{\delta(1 - x^*)}{(\delta + x^*)}$, $J_2 = -\dfrac{\alpha\delta\gamma}{\beta(\delta + y^*)} < 0$, $J_3 = \dfrac{\epsilon\beta\delta(1 - x^*)}{\alpha(\delta + x^*)} > 0$, and $J_4 = \epsilon\gamma[\dfrac{\delta}{(\delta + y^*)} - 1] < 0$.

Using the Routh-Hurwitz criteria, it can be judged that $E_3(x^*, y^*)$ is asymptotically stable if

$$J_1 + J_4 < 0, \ J_1 J_4 - J_2 J_3 > 0. \tag{3.5}$$

Theorem 3.1. *The unique positive equilibra $E_3(x^*, y^*)$ is asymptotically stable if*

$$\delta > 1 - 2x^*. \tag{3.6}$$

We study the existence of Hopf bifurcation in a small neighborhood of $E_3(x^*, y^*)$, and choose δ as a bifurcation parameter. The characteristic equation of Jacobian matrix $J^*(x^*, y^*)$ can be written as

$$\lambda^2 - Tr(J^*)\lambda + det(J^*) = 0. \tag{3.7}$$

Mark the eigenvalues of E_3 as $\lambda(\delta) = \mu(\delta) \pm i\omega(\delta)$, where

$$\mu(\delta) = \frac{1}{2}Tr(J), \ \omega(\delta) = \frac{1}{2}\sqrt{Tr(J)^2 - 4det(J)}.$$

It is well known that $\mu(\delta) = 0$ and $\omega(\delta) > 0$ are necessary conditions for Hopf bifurcation to occur. Obviously, $Tr(J) = 0$ is equivalent to $\mu(\delta_0) = 0$, such as

$$\mu(\delta_0) = \frac{1}{2}Tr(J) = \frac{1}{2}\left(1 - 2x^* - \frac{\delta(1 - x^*)}{(\delta + x^*)} + \epsilon\gamma(\frac{\delta}{(\delta + y^*)} - 1)\right) = 0, \tag{3.8}$$

then we can derive

$$\delta_0 = \frac{1}{2x^*}\left(\sigma + \sqrt{\sigma^2 + 4x^*(x^*y^* - 2(x^*)^2y^* - x^*y^*\gamma\epsilon)}\right), \tag{3.9}$$

where $\sigma = x^* - 2(x^*)^2 - x^*y^* - y^*\gamma\epsilon$. Besides,

$$\mu'(\delta) = \frac{\delta(1 - x^*)}{(\delta + x^*)^2} - \frac{1 - x^*}{(\delta + x^*)} + \epsilon\gamma\frac{y^*}{(\delta + y^*)^2} = \frac{(x^* - 1)x^*}{(\delta + x^*)^2} + \epsilon\frac{\gamma y^*}{(\delta + y^*)^2} < 0. \tag{3.10}$$

Furthermore, $det(J) > 0$ is equivalent to $\omega(\delta) > 0$,

$$\begin{aligned} det(J) &= [1 - 2x^* - \frac{\delta(1-x^*)}{(\delta+x^*)}\epsilon\gamma(\frac{\delta}{(\delta+y^*)} - 1) + \frac{\epsilon\gamma\delta^2(1-x^*)}{(\delta+x^*)(\delta+y^*)}] \\ &= \frac{\epsilon\gamma(2x^*-1)y^*}{(\delta+y^*)} + \frac{\epsilon\gamma\delta(1-x^*)}{(\delta+x^*)} > 0. \end{aligned} \tag{3.11}$$

It is shown that Hopf bifurcation occurs when δ crosses δ_0, and the associated characteristic equation of system (2.4) has a pair of simple imaginary roots.

4. Direction and stability of the Hopf bifurcation

In the previous section, we have already obtained some conditions which ensure that system (2.5) experiences Hopf bifurcation at the unique positive equilibria $E_3(x^*, y^*)$ when δ takes the critical value δ_0. In this section, based on the center manifold theorem and the normal form theory, we will determine the direction, stability, and period of the bifurcation periodic solution produced by Hopf bifurcation.

We consider system

$$\begin{cases} \dfrac{\mathrm{d}x}{\mathrm{d}t} = x(1-x) - \dfrac{\alpha xy}{(\delta+x)(\delta+y)}, \\ \dfrac{\mathrm{d}y}{\mathrm{d}t} = \epsilon\left[\dfrac{\beta xy}{(\delta+x)(\delta+y)} - \gamma y\right]. \end{cases} \tag{4.1}$$

Let $\xi_1 = x - x^*,\ \xi_2 = y - y^*$, and we transform $E_3(x^*, y^*)$ into the origin. Then system (4.1) becomes

$$\begin{cases} \dfrac{\mathrm{d}\xi_1}{\mathrm{d}t} = (\xi_1 + x^*)(1 - \xi_1 - x^*) - \dfrac{\alpha(\xi_1+x^*)(\xi_2+y^*)}{(\delta+\xi_1+x^*)(\delta+\xi_2+y^*)}, \\ \dfrac{\mathrm{d}\xi_2}{\mathrm{d}t} = \epsilon\left[\dfrac{\beta(\xi_1+x^*)(\xi_2+y^*)}{(\delta+\xi_1+x^*)(\delta+\xi_2+y^*)} - \gamma(\xi_2+y^*)\right]. \end{cases} \tag{4.2}$$

We can write system (4.2) as

$$\begin{pmatrix} \xi_1' \\ \xi_2' \end{pmatrix} = J\begin{pmatrix} \xi_1 \\ \xi_2 \end{pmatrix} + \begin{pmatrix} f(\xi_1, \xi_2, \delta) \\ g(\xi_1, \xi_2, \delta) \end{pmatrix} \equiv J\xi + F, \tag{4.3}$$

where J is the Jacobian matrix of (4.2) at origin,

$$f = a_1\xi_1^2 + a_2\xi_1\xi_2 + a_3\xi_2^2 + a_4\xi_1^3 + a_5\xi_1^2\xi_2 + a_6\xi_1\xi_2^2 + a_7\xi_2^3 + O(|\xi_1+\xi_2|^4), \tag{4.4}$$

$$g = b_1\xi_1^2 + b_2\xi_1\xi_2 + b_3\xi_2^2 + b_4\xi_1^3 + b_5\xi_1^2\xi_2 + b_6\xi_1\xi_2^2 + b_7\xi_2^3 + O(|\xi_1+\xi_2|^4), \tag{4.5}$$

and

$$a_1 = -1 + \frac{\alpha\delta y^*}{(\delta + x^*)^3(\delta + y^*)},\ a_2 = -\frac{\alpha\delta^2}{(\delta + x^*)^2(\delta + y^*)^2},\ a_3 = \frac{\alpha\delta x^*}{(\delta + x^*)(\delta + y^*)^3},$$
$$a_4 = -\frac{\alpha\delta y^*}{(\delta + x^*)^4(\delta + y^*)},\ a_5 = \frac{\alpha\delta^2}{(\delta + x^*)^3(\delta + y^*)^2},\ a_6 = \frac{\alpha\delta^2}{(\delta + x^*)^2(\delta + y^*)^3},$$
$$a_7 = -\frac{\alpha\delta x^*}{(\delta + x^*)(\delta + y^*)^4},\ b_1 = -\frac{\epsilon\delta\beta y^*}{(\delta + x^*)^3(\delta + y^*)},\ b_2 = \frac{\epsilon\beta\delta^2}{(\delta + x^*)^2(\delta + y^*)^2},$$
$$b_3 = -\frac{\epsilon\beta\delta x^*}{(\delta + x^*)(\delta + y^*)^3},\ b_4 = \frac{\epsilon\beta\delta y^*}{(\delta + x^*)^4(\delta + y^*)},\ b_5 = -\frac{\epsilon\beta\delta^2}{(\delta + x^*)^3(\delta + y^*)^2},$$
$$b_6 = -\frac{\epsilon\beta\delta^2}{(\delta + x^*)^2(\delta + y^*)^3},\ b_7 = \frac{\epsilon\beta\delta x^*}{(\delta + x^*)(\delta + y^*)^4}.$$

The eigenvectors of matrix $J(\delta_0)$ are

$$p = \begin{pmatrix} \dfrac{-i\omega(\delta)}{2\alpha R} \\ 1 \end{pmatrix}, \quad q = \begin{pmatrix} \dfrac{i\omega(\delta)}{2\alpha R} \\ 1 \end{pmatrix}.$$

Vectors p, q satisfy

$$Jq = i\omega(\delta_0)q,\ J^T p = -i\omega(\delta_0)p. \tag{4.6}$$

In the following, we adopt the method of Hassard [4] to compute the coordinates to describe the center manifold C_0 at $\delta = \delta_0$. System (4.3) can be written as

$$\dot{\xi} = J\xi + \frac{1}{2}B(\xi, \eta) + \frac{1}{6}C(\xi, \eta, \zeta). \tag{4.7}$$

Generally, $J = J(\delta_0)$. B and C are symmetric multilinear functions valued by plane vectors $\xi = (\xi_1, \xi_2)^T$, $\eta = (\eta_1, \eta_2)^T$, and $\zeta = (\zeta_1, \zeta_2)^T$, and their coordinates are given later. Define

$$z =< p, \xi >,\ \dot{z} = \lambda(\delta)z + g(z, \bar{z}, \delta). \tag{4.8}$$

On the center manifold C_0, we have

$$W(t, \theta) = W(z(t), \bar{z}(t), \theta), \tag{4.9}$$

where

$$W(z, \bar{z}, \theta) = W_{20}(\theta)\frac{z^2}{2} + W_{11}(\theta)z\bar{z} + W_{02}(\theta)\frac{\bar{z}^2}{2} + W_{30}(\theta)\frac{z^3}{6} + \cdots.$$

z and $\bar{z}$ are local coordinates for center manifold C_0. Note that W is real if $\xi(t)$ is real. We consider only real solutions. For the solution $\xi(t) \in C_0$ of (4.7), since $\delta = \delta_0$, we have

$$\dot{z} = \lambda(\delta)z + \langle p(\delta), F(zq(\delta) + \bar{z}\bar{q}(\delta), \delta)\rangle. \tag{4.10}$$

We rewrite this equation as

$$\dot{z}(t) = \lambda(\delta)z(t) + g(z, \bar{z}, \delta), \tag{4.11}$$

with

$$g(z, \bar{z}, \delta) = \langle p(\delta), F(zq(\delta) + \bar{z}\bar{q}(\delta), \delta)\rangle. \tag{4.12}$$

According to Section 3.3 of Kuznetsov [8], we know that g can be written as a Taylor series in the form of two complex variables(z and $\bar{z}$),

$$g(z,\bar{z},\delta)=\sum_{k+l\geqslant 2}\frac{1}{k!l!}g_{kl}(\delta)z^k\bar{z}^l, \tag{4.13}$$

where $g_{kl}(\delta)=\dfrac{\partial^{k+l}}{\partial z^k\partial\bar{z}^l}\langle p(\delta),F(zq(\delta)+\bar{z}\bar{q}(\delta),\delta)\rangle\Big|_{z=0}$, for $k+l\geq 2,\ k,l=0,1,\cdots$. For $\delta=\delta_0$, we can know

$$g(z,\bar{z},\delta)=g_{20}\frac{z^2}{2}+g_{11}z\bar{z}+g_{02}\frac{\bar{z}^2}{2}+g_{21}\frac{z^2\bar{z}}{2}+\cdots \tag{4.14}$$

by (4.13).

Now using the process described in [8], we give the coordinate representation of a symmetric multilinear function $B(\xi,\eta)$ and $C(\xi,\eta,\zeta)$ in detail,

$$B(\xi,\eta)=\begin{pmatrix}\sum\limits_{i,j=1}^{2}\dfrac{\partial^2F_1(\xi,0)}{\partial\xi_i\partial\xi_j}|_{\xi=\mathbf{0}}\ \xi_i\eta_j\\ \sum\limits_{i,j=1}^{2}\dfrac{\partial^2F_2(\xi,0)}{\partial\xi_i\partial\xi_j}|_{\xi=\mathbf{0}}\ \xi_i\eta_j\end{pmatrix}=\begin{pmatrix}2a_1\xi_1\eta_1+a_2\xi_1\eta_2+a_2\xi_2\eta_1+2a_3\xi_2\eta_2\\ 2b_1\xi_1\eta_1+b_2\xi_1\eta_2+b_2\xi_2\eta_1+2b_3\xi_2\eta_2\end{pmatrix}, \tag{4.15}$$

$$\begin{aligned}C(\xi,\eta,\zeta)&=\begin{pmatrix}\sum\limits_{i,j,k=1}^{2}\dfrac{\partial^3F_1(\xi,0)}{\partial\xi_i\partial\xi_j\partial\xi_k}|_{\xi=\mathbf{0}}\ \xi_i\eta_j\zeta_i\\ \sum\limits_{i,j,k=1}^{2}\dfrac{\partial^3F_2(\xi,0)}{\partial\xi_i\partial\xi_j\partial\xi_k}|_{\xi=\mathbf{0}}\ \xi_i\eta_j\zeta_i\end{pmatrix}\\ &=\begin{pmatrix}6a_4\xi_1\eta_1\zeta_1+2a_5\xi_1\eta_1\zeta_2+2a_5\xi_2\eta_1\zeta_1\\ +2a_6\xi_1\eta_2\zeta_1+2a_6\xi_1\eta_2\zeta_2+6a_7\xi_2\eta_2\zeta_2\\ 6b_4\xi_1\eta_1\zeta_1+2b_5\xi_1\eta_1\zeta_2+2b_5\xi_2\eta_1\zeta_1\\ +2b_6\xi_1\eta_2\zeta_1+2b_6\xi_1\eta_2\zeta_2+6b_7\xi_2\eta_2\zeta_2\end{pmatrix}.\end{aligned} \tag{4.16}$$

In addition, we can also get the relationship between B and z and $\bar{z}$,

$$B(zq+\bar{z}\bar{q},zq+\bar{z}\bar{q})=z^2B(q,q)+2z\bar{z}B(q,\bar{q})+\bar{z}^2B(\bar{q},\bar{q}), \tag{4.17}$$

in which $q=q(0)$ and $p=p(0)$. Therefore, the Taylor coefficient g_{kl}, $k+l=2$ of the quadratic term in $g(z,\bar{z},\delta)$ can be expressed by the following formula

$$g_{20}=\langle p,B(q,q)\rangle,\quad g_{11}=\langle p,B(q,\bar{q})\rangle,\quad g_{02}=\langle p,B(\bar{q},\bar{q})\rangle.$$

Similarly, compute C to get

$$g_{21}=\langle p,C(q,q,\bar{q})\rangle.$$

After calculation, it can be easily obtained that

$$g_{20}=<p,B(q,q)>=\frac{ia_1\omega^3}{4\alpha^3R^3}-\frac{(b_1+a_2)\omega^2}{2\alpha^2R^2}-\frac{i(b_2+a_3)\omega}{2\alpha R}+2b_3, \tag{4.18}$$

$$g_{02} =< p, B(\overline{q}, \overline{q}) >= \frac{ia_1\omega^3}{4\alpha^3R^3} - \frac{(b_1 - a_2)\omega^2}{2\alpha^2R^2} - \frac{i(b_2 + a_3)\omega}{2\alpha R} + 2b_3, \tag{4.19}$$

$$g_{11} =< p, B(q, \overline{q}) >= -\frac{ia_1\omega^3}{4\alpha^3R^3} - \frac{ia_3\omega}{\alpha R} + \frac{b_1\omega}{2\alpha^2R^2} + 2b_3, \tag{4.20}$$

$$g_{21} =< p, C(q, q, \overline{q}) >= \frac{3ia_4\omega^3}{4\alpha^3R^3} + 6a_7. \tag{4.21}$$

Finally, the following parameters can be calculated to determine the nature of the Hopf bifurcation:

$$C_1(0) = \frac{i}{2\omega_0}\left(g_{20}g_{11} - 2|g_{11}|^2 - \frac{1}{3}|g_{02}|^2\right) + \frac{g_{21}}{2}, \tag{4.22}$$

$$\rho = -\frac{Re\{C_1(0)\}}{Re\{\lambda'(\delta_0)\}}, \tag{4.23}$$

$$\theta = 2Re\{C_1(0)\}, \tag{4.24}$$

$$T_2 = -\frac{Im\{C_1(0)\} + \rho Im\{\lambda'(\delta_0)\}}{\omega_0}. \tag{4.25}$$

The sign of the above notations can show the properties of the Hopf bifurcation. We know that the Hopf bifurcation is termed supercritical if $\rho > 0$ and subcritical if $\rho < 0$; the periodic solutions on the center manifold are stable if $\theta < 0$ and are unstable if $\theta > 0$; the period of the bifurcation periodic solution increase if $T_2 > 0$, and the period decrease if $T_2 < 0$. From the previous discussion, we know that $Re\{\lambda'(\delta_0)\} = \mu'(\delta_0) < 0$, therefore we can get the following result.

Theorem 4.1. *The direction and stability of the Hopf Bifurcation are determined by the sign of* $Re\{C_1(0)\}$. *The direction of the Hopf bifurcation of system(2.4) is supercritical (subcritical) and the bifurcating periodic solutions on the center manifold are unstable (stable) if* $Re\{C_1(0)\} > 0$ (< 0).

5. Flip bifurcation

In the actual ecosystem, it is sometimes necessary to discretize the system model, which can facilitate our obtaining of biological data. Since the original system is a two-dimensional nonlinear system, we cannot study the dynamics of the system by obtaining its analytical solution. The forward Euler method is used to obtain the discrete dynamic system to better study the dynamic behavior of the system.

In this section, we still choose δ as the bifurcation parameter. We will use the central manifold and bifurcation theory to discuss the flip bifurcation at $E_3(x^*, y^*)$, as described in [3, 16, 25].

We consider the system

$$\begin{cases} x(n+1) = x(n) + x(n)(1 - x(n)) - \dfrac{\alpha x(n)y(n)}{(\delta + x(n))(\delta + y(n))} \\ y(n+1) = y(n) + \epsilon\left[\dfrac{\beta x(n)y(n)}{(\delta + x(n))(\delta + y(n))} - \gamma y(n)\right] \end{cases}. \tag{5.1}$$

Map (5.1) has a unique interior fixed point $E_3(x^*, y^*)$, at which the eigenvalues are

$$\lambda_1 = -1, \ \lambda_2 = \frac{Tr(J^*) + \sqrt{Tr(J^*)^2 - 4det(J_*)}}{2},$$

with $|\lambda_2| \neq 1$. For $|\delta^*| \ll 1$, we consider a perturbation of map (5.1) as follows:

$$\begin{cases} x(n+1) = x(n) + x(n)(1-x(n)) - \dfrac{\alpha x(n)y(n)}{(\delta+\delta^*+x(n))(\delta+\delta^*+y(n))} \equiv f_1(x,y) \\ y(n+1) = y(n) + \epsilon(\dfrac{\beta x(n)y(n)}{(\delta+\delta^*+x(n))(\delta+\delta^*+y(n))} - \gamma y(n)) \equiv f_2(x,y) \end{cases}, \tag{5.2}$$

where δ^* is a perturbation parameter.

Let $u = x - x^*$, $v = y - y^*$, and transform $E_3(x^*, y^*)$ into the origin. Then map (5.2) becomes

$$\begin{pmatrix} u \\ v \end{pmatrix} \to \begin{pmatrix} a_{11}u + a_{12}v + a_{13}u^2 + a_{14}uv + a_{15}v^2 + c_{11}u\delta^* + c_{12}v\delta^* + c_{13}u^2\delta^* \\ +c_{14}uv\delta^* + c_{15}v^2\delta^* + d_1u^3 + d_2u^2v + d_3uv^2 + d_4v^3 + O(|u+v+\delta^*|^4) \\ a_{21}u + a_{22}v + a_{23}u^2 + a_{24}uv + a_{25}v^2 + c_{21}u\delta^* + c_{22}v\delta^* + c_{23}u^2\delta^* \\ +c_{24}uv\delta^* + c_{25}v^2\delta^* + e_1u^3 + e_2u^2v + e_3uv^2 + e_4v^3 + O(|u+v+\delta^*|^4) \end{pmatrix},$$

where $a_{i1} + c_{i1}\delta^* = \dfrac{\partial f_i}{\partial x}$, $a_{i2} + c_{i2}\delta^* = \dfrac{\partial f_i}{\partial y}$, $a_{i3} + c_{i3}\delta^* = \dfrac{\partial^2 f_i}{\partial x^2}$, $a_{i4} + c_{i4}\delta^* = \dfrac{\partial^2 f_i}{\partial x \partial y}$, $a_{i5} + c_{i5}\delta^* = \dfrac{\partial^2 f_i}{\partial y^2}$, $i = 1, 2$, and

$$d_1 = \frac{\partial^3 f_1}{\partial x^3}, d_2 = \frac{\partial^3 f_1}{\partial x^2 \partial y}, d_3 = \frac{\partial^3 f_1}{\partial x \partial y^2}, \ d_4 = \frac{\partial^3 f_1}{\partial y^3},$$

$$e_1 = \frac{\partial^3 f_2}{\partial x^3}, e_2 = \frac{\partial^3 f_2}{\partial x^2 \partial y}, e_3 = \frac{\partial^3 f_2}{\partial x \partial y^2}, \ e_4 = \frac{\partial^3 f_2}{\partial y^3}.$$

c_{ij} are the terms containing δ^*; a_{ij} and d_{ij} are the terms that do not contain δ^*.

Construct an matrix

$$T = \begin{pmatrix} a_{12} & a_{12} \\ -1 - a_{11} & \lambda_2 - a_{11} \end{pmatrix}. \tag{5.3}$$

Then we use the translation

$$\begin{pmatrix} u \\ v \end{pmatrix} = T \begin{pmatrix} \tilde{x} \\ \tilde{y} \end{pmatrix}, \tag{5.4}$$

and the map (5.1) becomes

$$\begin{pmatrix} \tilde{x} \\ \tilde{y} \end{pmatrix} \to \begin{pmatrix} -1 & 0 \\ 0 & \lambda_2 \end{pmatrix} \begin{pmatrix} \tilde{x} \\ \tilde{y} \end{pmatrix} + \begin{pmatrix} \tilde{f}(x,y,\delta^*) \\ \tilde{g}(x,y,\delta^*) \end{pmatrix}, \tag{5.5}$$

where

$$\begin{aligned}\tilde{f}(x,y,\delta^*) =&\frac{a_{13}(\lambda_2-a_{11})-a_{12}a_{23}}{a_{12}(\lambda_2+1)}u^2+\frac{a_{14}(\lambda_2-a_{11})-a_{12}a_{24}}{a_{12}(\lambda_2+1)}uv\\&+\frac{a_{15}(\lambda_2-a_{11})-a_{12}a_{25}}{a_{12}(\lambda_2+1)}v^2+\frac{c_{11}(\lambda_2-a_{11})-a_{12}c_{12}}{a_{12}(\lambda_2+1)}u\delta^*\\&+\frac{c_{12}(\lambda_2-a_{11})-a_{12}c_{22}}{a_{12}(\lambda_2+1)}v\delta^*+\frac{c_{13}(\lambda_2-a_{11})-a_{12}c_{23}}{a_{12}(\lambda_2+1)}u^2\delta^*\\&+\frac{c_{14}(\lambda_2-a_{11})-a_{12}c_{24}}{a_{12}(\lambda_2+1)}uv\delta^*+\frac{c_{15}(\lambda_2-a_{11})-a_{12}c_{25}}{a_{12}(\lambda_2+1)}v^2\delta^*\\&+\frac{d_1(\lambda_2-a_{11})-a_{12}e_1}{a_{12}(\lambda_2+1)}u^3+\frac{d_2(\lambda_2-a_{11})-a_{12}e_2}{a_{12}(\lambda_2+1)}u^2v\\&+\frac{d_3(\lambda_2-a_{11})-a_{12}e_3}{a_{12}(\lambda_2+1)}uv^2+\frac{d_4(\lambda_2-a_{11})-a_{12}e_4}{a_{12}(\lambda_2+1)}v^3\\&+O((|u|+|v|+|\delta^*|)^4),\end{aligned}$$

$$\begin{aligned}\tilde{g}(x,y,\delta^*) =&\frac{a_{13}(1+a_{11})+a_{12}a_{23}}{a_{12}(\lambda_2+1)}u^2+\frac{a_{14}(1+a_{11})+a_{12}a_{24}}{a_{12}(\lambda_2+1)}uv\\&+\frac{a_{15}(1+a_{11})+a_{12}a_{25}}{a_{12}(\lambda_2+1)}v^2+\frac{c_{11}(1+a_{11})+a_{12}c_{12}}{a_{12}(\lambda_2+1)}u\delta^*\\&+\frac{c_{12}(1+a_{11})+a_{12}c_{22}}{a_{12}(\lambda_2+1)}v\delta^*+\frac{c_{13}(1+a_{11})+a_{12}c_{23}}{a_{12}(\lambda_2+1)}u^2\delta^*\\&+\frac{c_{14}(1+a_{11})+a_{12}c_{24}}{a_{12}(\lambda_2+1)}uv\delta^*+\frac{c_{15}(1+a_{11})+a_{12}c_{25}}{a_{12}(\lambda_2+1)}v^2\delta^*\\&+\frac{d_1(1+a_{11})-a_{12}e_1}{a_{12}(\lambda_2+1)}u^3+\frac{d_2(1+a_{11})+a_{12}e_2}{a_{12}(\lambda_2+1)}u^2v\\&+\frac{d_3(1+a_{11})+a_{12}e_3}{a_{12}(\lambda_2+1)}uv^2+\frac{d_4(1+a_{11})+a_{12}e_4}{a_{12}(\lambda_2+1)}v^3\\&+O((|u|+|v|+|\delta^*|)^4),\end{aligned}$$

and

$$\begin{aligned}u =&a_{12}(\tilde{x}+\tilde{y}),\ v=-(1+a_{11})\tilde{x}+(\lambda_2-a_{11})\tilde{y},\ u^2=a_{12}^2(\tilde{x}^2+2\tilde{x}\tilde{y}+\tilde{y}^2),\\uv =&-a_{12}(1+a_{11})\tilde{x}^2+a_{12}(\lambda_2-1-2a_{11})\tilde{x}\tilde{y}+a_{12}(\lambda_2-a_{11})\tilde{y}^2,\\v^2 =&(1+a_{11})^2\tilde{x}^2-2(1+a_{11})(\lambda_2-a_{11})\tilde{x}\tilde{y}+(\lambda_2-a_{11})^2\tilde{y}^2,\\u^3 =&a_{12}^3(\tilde{x}^3+3\tilde{x}^2\tilde{y}+3\tilde{x}\tilde{y}^2+\tilde{y}^3),\\u^2v =&a_{12}^2[-(1+a_{11})\tilde{x}^3+(\lambda_2-2-3a_{11})\tilde{x}^2\tilde{y}+(2\lambda_2-1-3a_{11})\tilde{x}\tilde{y}^2+(\lambda_2-a_{11})\tilde{y}^3],\\uv^2 =&a_{12}[(1+a_{11})^2\tilde{x}^3+(1-\lambda_2+3a_{11})(1+a_{11})\tilde{x}^2\tilde{y}+(\lambda_2-a_{11})^2\tilde{y}^3\\&+(\lambda_2-2-3a_{11})(\lambda_2-a_{11})\tilde{x}\tilde{y}^2],\\v^3 =&-(1+a_{11})^3\tilde{x}^3+3(1+a_{11})^2(\lambda_2-a_{11})\tilde{x}^2\tilde{y}-3(1+a_{11})(\lambda_2-a_{11})^2\tilde{x}\tilde{y}^2\\&+(\lambda_2-a_{11})^3\tilde{y}^3.\end{aligned}$$

Next, we determine a center manifold $W^c(0,0,0)$ of map (5.5) at the fixed point $(0,0)$ in a small neighborhood of $\delta^*=0$. From the center manifold theorem [8], we

know that there exists a center manifold $W^c(0,0,0)$, which can be approximately represented as follows:

$$W^c(0,0,0)=\{(\tilde{x},\tilde{y},\delta^*)\in R^3:\tilde{y}=k_1\tilde{x}^2+k_2\tilde{x}\delta^*+k_3{\delta^*}^2+O((|\tilde{x}|+|\delta^*|)^3)\}.$$

By calculation, we get

$$k_1=\frac{a_{12}[a_{13}(1+a_{11})+a_{12}a_{23}]+(1+a_{11})[(a_{25}-a_{14})(1+a_{11})-a_{12}a_{24}]}{1-\lambda_2^2},$$
$$k_2=\frac{(1+a_{11})[c_{12}(1+a_{11})+a_{12}c_{22}]-a_{12}[c_{11}(1+a_{11})+a_{12}c_{21}]}{a_{12}(1+\lambda_2)^2},\ k_3=0.$$

Therefore, we consider the map (5.5) which is restricted to the center manifold $W^c(0,0,0)$:

$$F_1:\tilde{x}\to-\tilde{x}+h_1\tilde{x}^2+h_2x\delta^*+h_3\tilde{x}^2\delta^*+h_4\tilde{x}{\delta^*}^2+h_5\tilde{x}^3+O((|\tilde{x}|+|\delta^*|)^4),\quad(5.6)$$

where

$$\begin{aligned}
h_1=&\frac{1}{\lambda_2+1}\{a_{12}[a_{13}(\lambda_2-a_{11})-a_{12}a_{23}]-(1+a_{11})[a_{14}(\lambda_2-a_{11})-a_{12}a_{24}]\\
&-a_{25}(1+a_{11})^2\},\\
h_2=&\frac{1}{a_{12}(\lambda_2+1)}\{a_{12}[c_{11}(\lambda_2-a_{11})-a_{12}c_1]-(1+a_{11})[c_{12}(\lambda_2-a_{11})-a_{12}c_{22}],\\
h_3=&\frac{a_2}{(\lambda_2+1)}\{2a_{12}[a_{13}(\lambda_2-a_{11})-a_{12}a_{23}]+(\lambda_2-1-2a_{11})[a_{14}(\lambda_2-a_{11})-a_{12}a_{24}]\\
&+\frac{a_1}{a_{12}(\lambda_2+1)}\{a_{12}[c_{11}(\lambda_2-a_{11})-a_{12}c_{21}]+(\lambda_2-a_{11})[c_{12}(\lambda_2-a_{11})-a_{12}c_{22}]\}\\
&+\frac{1}{\lambda_2+1}\{2a_{22}a_{25}(1+a_{11})(\lambda_2-a_{11})+a_{12}[c_{13}(\lambda_2-a_{11})-a_{12}c_{23}]\\
&-(1+a_{11})[c_{14}(\lambda_2-a_{11})-a_{12}c_{24}]-c_{25}(1+a_{11})^2\},\\
h_4=&\frac{a_1}{a_{12}(\lambda_2+1)}\{a_{12}[c_{11}(\lambda_2-a_{11})-a_{12}c_{21}]+(\lambda_2-a_{11})[c_{12}(\lambda_2-a_{11})-a_{12}c_{22}],\\
h_5=&\frac{1}{\lambda_2+1}\{2a_{12}a_{11}[a_{13}(\lambda_2-a_{11})-a_{12}a_{23}]+a_{11}(\lambda_2-1-2a_{11})[a_{14}(\lambda_2-a_{11})\\
&-a_{12}a_{24}]+a_{12}^2[d_1(\lambda_2-a_{11})-a_{12}e_1]-a_{12}(1+a_{11})[d_2(\lambda_2-a_{11})-a_{12}e_2]\\
&+2a_{11}a_{25}(1+a_{11})(\lambda_2-a_{11})-d_3a_{12}(1+a_{11})^2\}.
\end{aligned}$$

In order to make the map (5.5) undergo a flip bifurcation, we give that two discriminatory quantities α_1 and α_2 and require them to be non-zero where

$$\begin{aligned}
\alpha_1&=\left(\frac{\partial^2F_1}{\partial x\partial\delta^*}+\frac{1}{2}\frac{\partial^2F_1}{\partial\delta^*}\frac{\partial^2F_1}{\partial x^2}\right)|_{(0,0)}=h_2\neq0,\\
\alpha_2&=\left(\frac{1}{6}\frac{\partial^3F_1}{\partial x^3}+(\frac{1}{2}\frac{\partial^2F_1}{\partial x^2})^2\right)|_{(0,0)}=h_5+h_1^2\neq0.
\end{aligned}\quad(5.7)$$

Combining the above analysis with the theorem in [3], we can get the following result.

Theorem 5.1. *If $\alpha_2\neq0$, then map (5.1) undergoes a flip bifurcation at the fixed point $E_3(x^*,y^*)$ when the parameter δ^* varies in a small neighborhood of origin. Furthermore, the period orbits that bifurcate from $E_3(x^*,y^*)$ are stable if $\alpha_2>0$, and the period orbits are unstable if $\alpha_2<0$.*

6. Numerical simulations

In this section, we will use a concrete numerical example of model (2.4) to illustrate the previous theoretical analysis results. We consider the parameter set as $\alpha = 0.8$, $\beta = 10$, $\gamma = 0.1$ and $\epsilon = 0.01$, that is,

$$\begin{cases} \dot{x} = x(1-x) - \dfrac{0.8xy}{(\delta+x)(\delta+y)}, \\ \dot{y} = 0.01(\dfrac{10xy}{(\delta+x)(\delta+y)} - 0.1y), \end{cases} \tag{6.1}$$

with different random initial conditions.

Especially, we first consider the situation where the system (6.1) can reach a steady state when $\delta = 0.9$. The equilibrium abundance of prey and predator as $x^* = 0.3849$, $y^* = 29.0549$ can be calculated. The above parameters can satisfy the conditions given in Lemma 3.1 and Theorem 3.1. Thus, the equilibrium point $E^* = (0.3849, 29.0549)$ is asymptotically stable.

As shown in the figures, the system converges to the equilibrium point

$$E^* = (0.3769, 29.3540)$$

with any initial value(see Fig. 1). Alternatively, the system generates periodic solutions with any initial value(see Fig. 2).

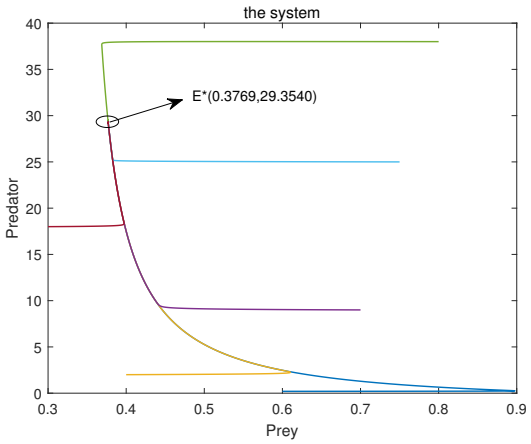

Figure 1. The positive equilibrium of system (2.4) is globally asymptotically stable with different initial values when $\delta > \delta_0$.

As shown in Fig. 1, for the equilibrium point $E_3(x^*, y^*)$, there is a slight difference between the value $E^* = (0.3769, 29.3540)$ obtained by MATLAB simulation and our calculation $E_3 = (0.3849, 29.0549)$, which we consider to be within a reasonable range of numerical error.

Next, for the sake of completeness of the results, we consider the impact of two parameters α and β on the dynamic behaviors of the system. Take the values of other parameters with $\delta = 0.9$, $\epsilon = 0.01$, $\gamma = 0.1$, $\alpha = 10, 2.0, 1.1$ (Fig. 3) and $\beta = 10, 1.0, 0.4$ (Fig. 4).

Applying the previous results, one can determine the value of ρ, θ and T_2 at $\delta = \delta_0$. For the parameter set above, δ takes a critical value 0.7529. Fig. 1 presents

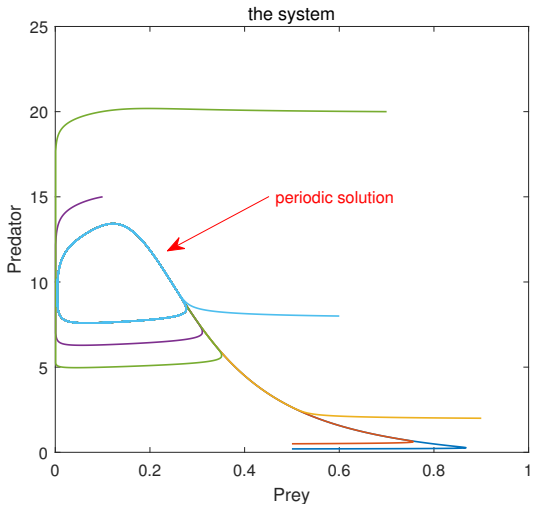

Figure 2. The system (2.4) has single periodic solution with different initial values when $\delta < \delta_0$.

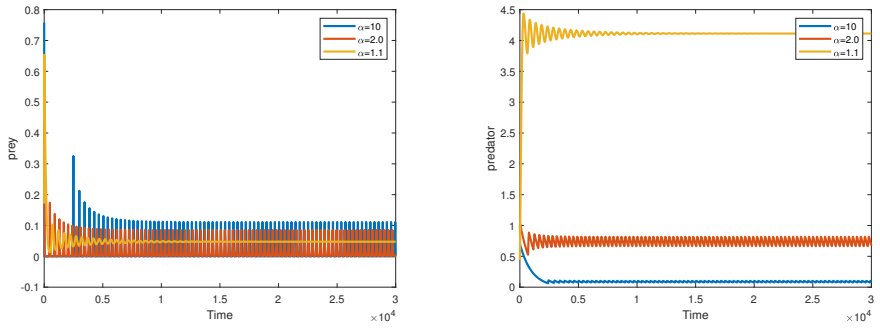

(a) Prey-time (b) Predator-time

Figure 3. Time series of x, y for different values of α. These two figures show that the system is unstable under that choice of parameters. Parameters are as in the text.

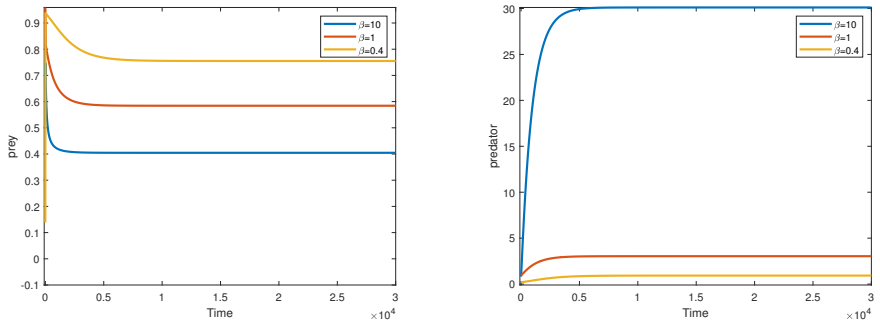

(a) Prey-time (b) Predator-time

Figure 4. Time series of x, y for different values of β. These two figures show that the system is absolutely stable under that choice of parameters. Parameters are as in the text.

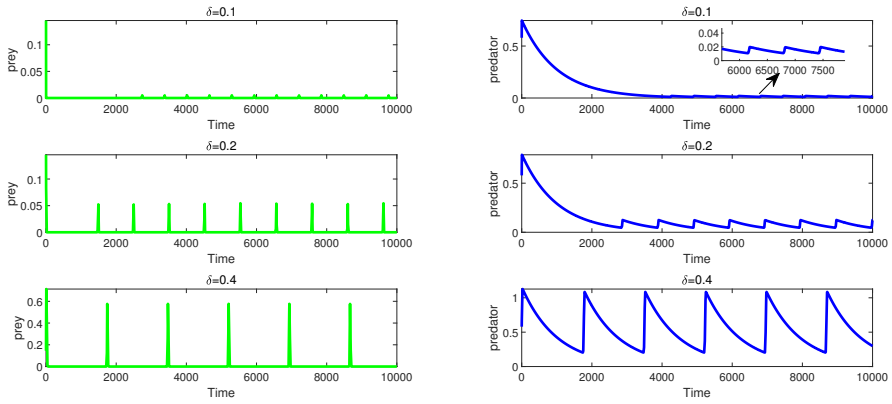

(a) Prey-time (b) Predator-time

Figure 5. The period of bifurcation periodic solution of predator population increases with δ, and the status of the predator is similar.

that, the system converges to the unique equilibrium point $E^* = (0.3769, 29.3540)$ with any initial value when $\delta > 0.7529$. When $\delta < 0.7529$, the system generates periodic solutions with any initial value (see Fig. 2). One can evaluate that $C_1(0) = -1.48399 \times 10^8 - 1.23169 \times 10^{11} i$, $\rho = -1.63191 \times 10^9 (< 0)$, $\theta = -2.96797 \times 10^8 (< 0)$ and $T_2 = 8.51391 \times 10^{12} (> 0)$. Since $\rho < 0$, Hopf bifurcation is subcritical and the bifurcating periodic solutions exist when $\delta < \delta_0$. Also, the bifurcating periodic solutions are stable as $\theta < 0$, and their period increases with δ as $T_2 > 0$, which can be observed from Fig. 5. When $\delta = 0.1$, the period is less than 1000; when $\delta = 0.2$, the period is close to 1000; when $\delta = 0.4$, the period is much greater than 1000.

7. Conclusions

In this paper, we considered a special predator-prey model with Crowley-Martin functional response, which has a small parameter ϵ. The local stability of the equilibrium points which are four boundary points and one positive point, has been analysed using the characteristic equation and the Routh-Hurwitz criterion. This paper determined the bifurcation parameter of the predator-prey system as δ through mathematical analysis of the system model.

We have found that under conditions (2.15) and (3.6), the solutions lose their stability and generate Hopf bifurcation with δ fluctuatin. When δ passes a critical value δ_0 from right to left, the family of periodic solutions bifurcates from equilibrium. Furthermore, using the center manifold theorem and normal form theory, the stability and direction of the Hopf bifurcation are determined. This paper has shown that when conditions (3.10) and (3.11) are established, the direction of Hopf bifurcation and the stability of the bifurcating periodic solutions of system (2.4) at δ_0 are determined by the sign of $Re\{C_1(0)\}$. We also analysed how the discrete system produces flip bifurcation.

Numerical results prove that the system converges to an equilibrium state when $\delta > \delta_0$; the system will appear Hopf bifurcation and produce bifurcation periodic

solutions when δ crosses δ_0; the solutions are stable when $\delta = \delta_0$. The Hopf bifurcation produced by the example given in the paper is subcritical. The bifurcating periodic solutions are stable, and its period increases with δ.

References

[1] P. Crowley, E. Martin, *Functional responses and interference within and between year classes of a dragonfly population*, Journal of the North American Benthological Society, 1989, 8(3), 211–221.

[2] D. Gray, J. Régnière, and B. Boulet, *Analysis and use of historical patterns of spruce budworm defoliation to forecast outbreak patterns in quebec*, Forest Ecology and Management, 2000, 127 (1-3), 217–231.

[3] J. Guckenheimer and P. Holmes, *Nonlinear Oscillations, Dynamical Systems, and Bifurcations of Vector Fields*, Springer Science & Business Media, Britain, 2013.

[4] B.D. Hassard, B. Hassard, N.D. Kazarinoff, Y.H. Wan, and Y.W. Wan, *Theory and Applications of Hopf Bifurcation*, Cambridge University Press, Cambridge, 1981.

[5] D. Jana, R. Pathak and M. Agarwal, *On the stability and hopf bifurcation of a prey-generalist predator system with independent age-selective harvesting*, Chaos, Solitons & Fractals, 2016, 83, 252–273.

[6] Y. Kuang, *Rich dynamics of gause-type ratio-dependent predator-prey system*, Fields Institute Communications, 1999, 21, 325–337.

[7] Y. Kuang and H. Freedman, *Uniqueness of limit cycles in gause-type models of predator-prey systems*, Mathematical Biosciences, 1988, 88(1), 67–84.

[8] Y. Kuznetsov, *Elements of Applied Bifurcation Theory*, Springer Science & Business Media, Berlin, 2013.

[9] X. Li, X. Lin and J. Liu, *Existence and global attractivity of positive periodic solutions for a predator-prey model with crowley-martin functional response*, Electronic Journal of Differential Equations, 2018, 191, 1–17.

[10] X. Liu, S. Zhong, B. Tian and F. Zheng, *Asymptotic properties of a stochastic predator-prey model with crowley-martin functional response*, Journal of Applied mathematics and computing, 2013, 43, 479–490.

[11] D. Ludwig, D. Jones and C. Holling, *Qualitative analysis of insect outbreak systems: the spruce budworm and forest*, The Journal of Animal Ecology, 1978, 41, 315–332.

[12] A. Maiti, B. Dubey and J. Tushar, *A delayed prey-predator model with Crowley-Martin-type functional response including prey refuge*, Mathematical Methods in the Applied Sciences, 2017, 40, 5792–5809.

[13] A.P. Maiti, B. Dubey, and A. Chakraborty, *Global analysis of a delayed stage structure prey–predator model with crowley–martin type functional response*, Mathematics and Computers in Simulation, 2019, 162, 58–84.

[14] N. Papanikolaou, N. Demiris, P. Milonas, S. Preston and T. Kypraios, *Does mutual interference affect the feeding rate of aphidophagous coccinellids? A modeling perspective*, PLoS One, 2016, 11, e0146168.

[15] A. Rasmussen, J. Wyller and J. Vik, *Relaxation oscillations in spruce-budworm interactions*, Nonlinear Analysis: Real World Applications, 2011, 12, 304–319.

[16] J. Ren, L. Yu and S. Siegmund, *Bifurcations and chaos in a discrete predator-prey model with Crowley-Martin functional response*, Nonlinear Dynamics, 2017, 90, 19–41.

[17] T. Saha, P. Pal and M. Banerjee, *Relaxation oscillation and canard explosion in a slow-fast predator-prey model with beddington-deangelis functional response*, Nonlinear Dynamics, 2021, 103, 1195–1217.

[18] P. Santra, G. Mahapatra, and G. Phaijoo, *Bifurcation and chaos of a discrete predator-prey model with crowley–martin functional response incorporating proportional prey refuge*, Mathematical Problems in Engineering, 2020, 2020(309814), 1–18.

[19] X. Shi, X. Zhou and X. Song, *Analysis of a stage-structured predator-prey model with crowley-martin function*, Journal of Applied Mathematics and Computing, 2011, 36, 459–472.

[20] G. Skalski and J Gilliam, *Functional responses with predator interference: viable alternatives to the holling type ii model*, Ecology, 2011, 82, 3083–3092.

[21] Y. Song and X. Zou, *Bifurcation analysis of a diffusive ratio-dependent predator-prey model*, Nonlinear Dynamics, 2014, 78, 49–70.

[22] T. Swetnam and A. Lynch, *Multicentury, regional-scale patterns of western spruce budworm outbreaks*, Ecological monographs, 1993, 63, 399–424.

[23] J. Tripathi, S. Tyagi and S. Abbas, *Global analysis of a delayed density dependent predator–prey model with crowley–martin functional response*, Communications in Nonlinear Science and Numerical Simulation, 2016, 30, 45–69.

[24] R. Upadhyay and R. Naji, *Dynamics of a three species food chain model with crowley-martin type functional response*, Chaos, solitons & fractals, 2009, 42, 1337–1346.

[25] S. Wiggins and M. Golubitsky, *Introduction to Applied Nonlinear Dynamical Systems and Chaos*, Springer, Berlin, 2003.

[26] J. Zhou, *Qualitative analysis of a modified leslie-gower predator-prey model with crowley-martin functional responses*, Communications on Pure & Applied Analysis, 2015, 14, 1127.